Evolution of fracture permeability in active clayey formations

Ali Seiphoori[1#], *Ulrich* Mok[2], and *Paul* Marschall[3]

[1]*Norwegian Geotechnical Institute (NGI), Advanced Geotechnical Testing Laboratory, 10615 Shadow Wood Dr., Suite 100, Houston, Texas, USA.*
[2]*Massachusetts Institute of Technology (MIT), Department of Earth, Atmospheric, and Planetary Sciences (EAPS), 77 Massachusetts Avenue, Cambridge, Massachusetts, USA.*
[3]*National Cooperative for Disposal of Radioactive Waste in Switzerland (NAGRA) Hardstrasse 73, 5430 Wettingen, Switzerland.*

[#]*Corresponding author: ali.seiphoori@ngi.no*

ABSTRACT

Opalinus Clay (OPA), a potential geological host formation for the disposal of high-level radioactive waste in Switzerland, is characterized by a low intrinsic permeability on the order of ~ 10^{-20} to 10^{-21} m^2. Nonetheless, its effective permeability can increase significantly due to active fractures, which are influenced by factors such as fracture geometry, solid-liquid interaction, and stress conditions. The evolution of the permeability and geometry of such active fractures, particularly in rocks containing swelling clay minerals, is important for assessing the long-term safety of the repositories. Here we present the results of an experimental investigation focused on understanding the evolution of permeability in fractured OPA. We employed an advanced high-pressure triaxial system to evaluate gas permeability, followed by a phase where gas was replaced with synthetic water. We observed a three-order-of-magnitude reduction in apparent permeability as fractures evolved, primarily due to active clay minerals and the associated swelling deformations. Furthermore, we conducted a detailed analysis of the material's internal pore structure at each stage of the experiment using X-ray computed tomography. Results may be used to understand the underlying processes in the evolution of fracture permeability in clayey formations applied in hydrocarbon reservoirs, carbon sequestration, and nuclear waste containment.

Keywords: Opalinus Clay; self-sealing; fractures permeability; radioactive waste storage.

1. Introduction

Self-sealing of fractures in clayey formations, including shale and claystone, is essential for the safe containment of nuclear waste within geological formations, effective carbon sequestration, and preserving the integrity of hydrocarbon reservoirs (Tsang et al., 2008; Bock et al., 2010; Elkhoury et al., 2015). The effective long-term isolation of radioactive waste or injected fluids necessitates geologic seals, or caprocks, with very low permeability. However, fractures induced by excavation in the host rock for geological waste disposal and fractures caused by fluid injection in carbon sequestration applications can form pathways that are orders of magnitude more conductive than the intact rock, potentially compromising the effectiveness of the seal.

In geological disposal of radioactive waste, formation of fracture networks, particularly the Excavation-Damaged Zone (EDZ, Figure 1), around the backfilled underground structures of a geological repository represents a release pathway for radionuclides, which needs to be addressed in the long-term safety assessment of the repositories (Mazurek et al., 2008; Bock et al., 2010; Bossart, 2018; Marschall et al., 2018). Conversely, the Excavation-Damaged Zone (EDZ) may serve as a highly efficient pathway for the release of gases resulting from corrosion and degradation of wastes (Diomidis, 2016; Johnson et al., 2004), which could help mitigate gas overpressures in the backfilled repository structures. The effectiveness of these release paths relies not only on the geometry of the EDZ but also on the 'self-sealing' capacity of the host rock formation and the prevailing stress state conditions, including *in-situ* stresses and pore pressure (Marschall et al., 2006, 2018). Self-sealing, or the reduction of fracture permeability arises from hydro-chemo-mechanical coupled processes primarily associated with the active clay components in argillaceous formations, which requires a mechanistic understanding of the intricate interaction between fluid and solid phases over time, a concept that is currently not fully understood.

This study is focused on characterizing the fracture permeability of Opalinus Clay to gas and the effectiveness of the self-sealing process following gas injection experiments, attributed to the swelling of clay minerals during re-saturation and hydration under general triaxial stress conditions. It aims to enhance our comprehension of flow and transport processes within the EDZ) of backfilled structures in a radioactive waste repository.

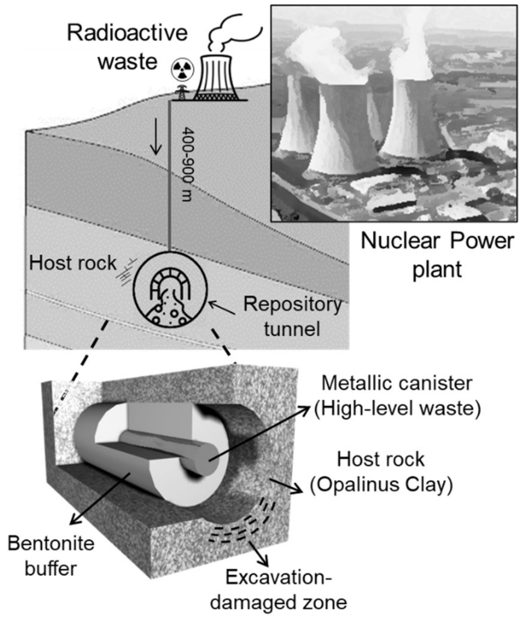

Figure 1. Geological disposal of high-level radioactive waste according to the Swiss concept. Fracture permeability within the Excavation-Damaged Zone (EDZ) is central to the long-term safety of the repository.

2. Materials and Methods

2.1. Opalinus Clay

Opalinus Clay is a sedimentary formation that can be classified as a claystone based on its mineralogical composition and a clayey siltstone based on its particle size analysis (Seiphoori et al., 2017). Originating around 174 – 170 million years ago in a marine environment, it was subjected to burial, uplift, and erosion processes (Mazurek et al. 2006).

Opalinus Clay materials were obtained from the Cement-clay Interaction (CI) experimental site of the Mont Terri Underground Research Laboratory (URL). The Mont Terri URL is located in the Jura Mountains of north-western Switzerland at a depth of approximately 250 – 300 meters. The Mont Terri Opalinus Clay was deposited in the Aalenian and was subjected to two successive stages of burial (in the Cretaceous and Tertiary) with a maximum burial depth of about 1'350 m during the Cretaceous, and 1'000 m during Miocene (Mazurek et al. 2006). Tectonic events during Alpine orogeny resulted in tilting and uplifting of the claystone strata, and in combination with erosion, caused the current state of over-consolidation (Bock 2000). The basic physical and geotechnical index characteristics of the Opalinus Clay used in this study are summarized in Table 1.

2.1.1. Mineralogy

We performed the bulk and < 2-micron clay fraction mineralogical analysis by X-ray powder diffraction (XRPD) presented in Figure 2. Clay minerals, including illite (I), illite-smectite mixed layer (IS), kaolinite, and chlorite, comprise ~68% of Opalinus Clay. The mineral composition of the IS mixed layer constitutes approximately 70% by weight of the clay fraction, indicating the significant swelling potential of Opalinus Clay upon hydration, which is central to fracture permeability and self-sealing behavior.

Table 1. Physical and index characteristics of Opalinus Clay (OPA).

In-situ depth (m)	300
Max. estimated depth (m)	1’350
Specific gravity, *Gs*	2.75
Water content, *w* (%)	6.95
Degree of saturation, S_r	95.6
Bulk density (g/cm^3)	2.44
Porosity, *n*	0.17

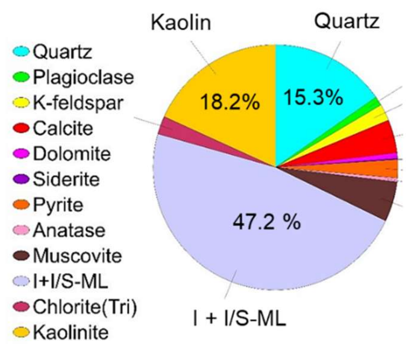

Figure 2. Mineralogical composition of the Opalinus Clay material from borehole BCI-21B, Mont Terri, studied in this research.

2.1.2. Microstructure

Figure 3 provides detailed information on the petrofabrics of Opalinus Clay and demonstrates their variability and heterogeneity.

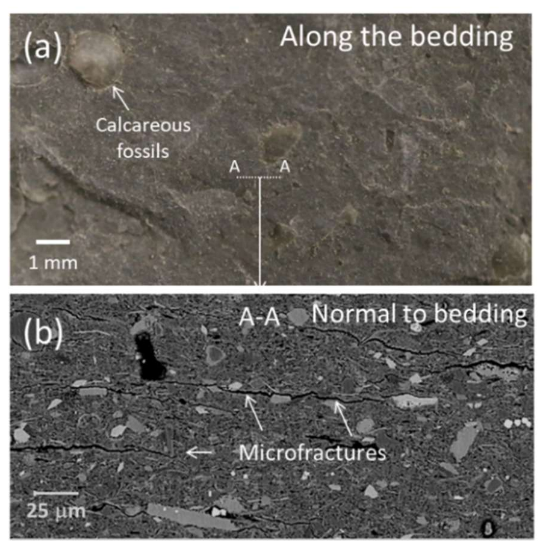

Figure 3. Microfabric of the Opalinus Clay material: (a) optical image of a broken surface along the bedding; (b) SEM photomicrograph of an ion-milled surface perpendicular to bedding.

The material displays a distinct microfabric characterized by clay aggregates and tabular-shaped non-clay particles, with a preferential orientation parallel to the fissility plane. Abundant inter-aggregate microfractures are evident, exhibiting a similar preferential orientation. Such microfractures caused by stress unloading during drilling and recovery (*i.e.,* tensile fractures) are likely the potential pathways for fluid flow and particle transport in Opalinus Clay.

2.2. Self-sealing Experiments

2.2.1. Sample preparation

Cylindrical samples (ratio 1:1; H≈D≈2") were prepared to investigate fracture permeability under triaxial loading conditions. Due to the presence of swelling clay minerals in Opalinus Clay, water cannot be applied during sample preparation and the process must be carried out under dry conditions. Intact cores were cut into smaller pieces with an abrasive bandsaw, and precision-cut into hexagonal prisms. These prisms were then trimmed into cylindrical samples using a lathe machine and a disk grinder. The resulting samples were subsequently sealed and stored for experimental purposes. We note that while fractures provided preferential flow paths, the permeability of well-mated tensile fractures subject to confining pressure typical of the formation depth was identified to be comparable to that of the intact material. Consequently, artificially fractured samples were prepared by employing an abrasive wire saw to cut the intact cylindrical samples in halves and form an unmated fracture along the bedding direction (Figure 4).

2.2.2. Triaxial testing

To assess the fracture permeability and self-sealing potential of Opalinus Clay, we utilized an advanced servo-hydraulic operated triaxial cell system (Autolab, 3000) from NER (New England Research, Inc.). This triaxial system incorporates a pressure vessel with an internal piston for differential (deviatoric) stress and servo-hydraulic pumps for pore fluid pressures. It offers precise control over confining pressures, pore pressure, flow rate, strain rate, and axial deviatoric load.

The pore pressure pumps provide testing with gas and water of varying chemical compositions. Moreover, the system is equipped with an acoustic emission module to measure ultrasonic compressional and shear wave velocities. Cylindrical samples were first copper-jacketed, where the jacket was secured to end platens using two Viton loops sealed with a flexible epoxy layer. Pre-compressed metallic mesh (#80) was used on both ends to prevent particle migration into the pore fluid system. The sample was then installed in the triaxial vessel and pressurized up to 10 MPa, ensuring copper jacket conformity onto the sample before instrumenting with strain gauges and acoustic sensors (see Figure 4). This process was required to ensure the integrity of the strain gauges and acoustic sensors when the sample was subject to larger stresses. We note that the OPA material from the Mont Terri site is highly over-consolidated (OCR≈4.5) with a maximum total stress of approximately 32.5 MPa undergone during the Cretaceous; thus, the applied stress is unlikely to modify the structure or impose a stress variation. Moreover, the diagenetic processes have further enhanced the strength and stiffness of the rock mass (Seiphoori et al., 2017). Local LVDTs were also installed on the sample to measure the total axial and radial deformation of the sample. The fully instrumented sample was then subject to gas and water flow to measure the fracture permeability under isotropic triaxial conditions. Before water saturation, the permeability of the fracture to Ar-gas was assessed through multiple cycles of isotropic loading/unloading. Beyond gas permeability, the fracture closure and creep effects were investigated.

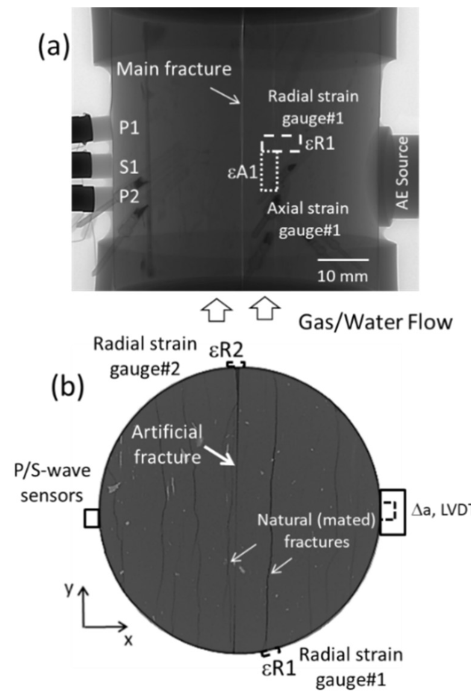

Figure 4. Cylindrical sample for self-sealing experiment via X-ray micro-CT images: (a) side view of the sample with artificial and natural fractures along the bedding plane; (b) top-view of the sample. "Δa, LVDT" refers to local measurements of the radial displacement normal to the bedding plane (H≈D≈2", where D is the diameter and H is the height of the sample).

3. Results

3.1. Gas permeability

The lithostatic stress (σ_p) and effective stress (σ_p') at this geological depth can be computed using the following equations (Seiphoori et al., 2017):

$$\sigma_p = [(1-\mathrm{n})G_s + n]\gamma_w h \quad (1)$$

$$\sigma_p' = (1-\mathrm{n})(G_s - 1)\gamma_w h \quad (2)$$

where n is the total porosity, G_s is the specific gravity, γ_w is the water unit weight, and h is the *in-situ* depth of the formation. Applying these equations, a total stress ranging from 12–22 MPa and an effective stress ranging from 7–14 MPa can be anticipated at the repository depth (500 – 900 m). The stresses applied during triaxial testing are consistent with the *in-situ* stresses estimated here, with a maximum confining stress of 16 MPa and a maximum pore water pressure reaching up to 3.8 MPa. We note that the pre-consolidation pressure of Opalinus Clay from Mont Terri is estimated to be approximately 13 MPa (Ferrari et al., 2016); therefore, we anticipate that the material primarily remains on the recompression curve within the range of applied effective stresses.

The permeability was measured under a steady-state condition using the automated *AutoLab* software incorporating the following equation:

$$\frac{Q}{A} = \frac{k}{\mu}\frac{\Delta p}{L} \quad (3)$$

where:

Q is the flow rate of the fluid (m^3/s), A is the cross-section of the sample (m^2), k is the permeability of a medium (m^2), μ is the dynamic viscosity of the fluid (Pa·s), ΔP is the applied pressure difference (Pa), and L is the length over which the pressure gradient acts (m).

The permeability of the fractured sample (or apparent permeability) to Ar-gas was assumed to be the steady-state permeability obtained using Equation (3). It was measured for multiple points during cycles of isotropic loading, unloading, and reloading, a gas pressure of 3.8 MPa, and the isotropic effective stress ($\sigma'_p = \sigma_p - u_{avg}$) ranging from 2.35 MPa to 12.45 MPa as presented in Figure 5. We note that a pressure difference of 1.4 – 2 MPa was applied for a duration of ~2 min for the steady-state gas-permeability measurements. The permeability averaged ~10^{-14}–10^{-15} m^2 approximately two orders of magnitude higher than that measured for the intact material. The average P-wave velocity of the intact material normal to the bedding plane was measured to be ~2400 m/s, approximately 500 m/s faster than that measured for the artificially fractured sample.

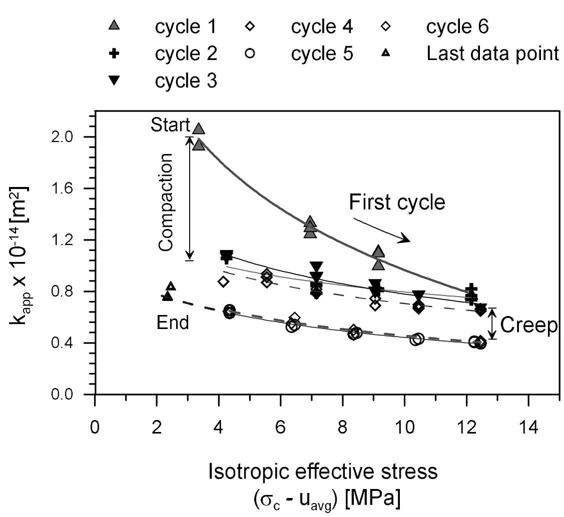

Figure 5. Evolution of apparent permeability of the fractured OPA to Ar-gas (u_{avg} = 3.8 MPa) during multiple cycles of loading, unloading, and reloading.

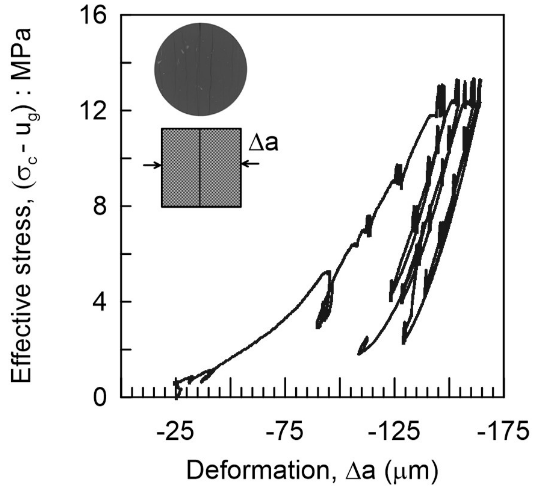

Figure 6. Aperture deformation measured by the LVDT locally installed perpendicular to the fracture plane during gas permeability experiments shown in Figure 5.

The main decline in fracture permeability was associated with the closure of the artificial fracture as well as natural fractures during the first cycle. Following the second cycle, the hysteresis effect became negligible. A hold time of approximately 17 hours post cycle 4 was applied to assess the impact of creep on permeability, leading to a subsequent decrease. Following cycles of loading, unloading, and reloading, the asperities stabilize, aligning with findings from previously reported research (e.g., Raven and Gale, 1985; Hofmann et al, 2016).

The deformation perpendicular to the fracture is gauged through the internal LVDT on the sample circumference during cycles of loading, unloading, and reloading (Figure 6). This variation primarily corresponds to the artificial fracture's aperture deformation and natural fracture closure. The total deformation includes both elastic and cumulative inelastic (plastic) strains as indicated in Figure 6.

3.2. Water permeability and self-sealing of fractures

To assess the self-sealing potential of Opalinus Clay, Ar-gas was replaced with synthetic water mimicking the in-situ pore liquid properties (see Mäder, 2011). After gas experiments, the total confining stress was maintained at 10 MPa, gas was evacuated by venting both pumps, where the pumps were subsequently filled with synthetic water. The bottom of the sample was then immediately flushed with water along the artificial fracture plane by applying a target pore pressure aiming at 3.8 MPa, facilitating the exit of gas from the sample through the top cap, which was vented to atmospheric conditions. The top cap pore pressure valve remained open until water flow was evident, at which point it was promptly closed, and pore water was introduced to the top of the sample. This procedure aimed at fracture saturation, preventing air entrapment within the fracture when the top of the sample was connected to the water flow. Subsequently, pore water pressures at both ends were raised to the target values of 3.8 MPa. To assess water permeability immediately after the initial fracture saturation, the top pore pressure was periodically reduced to 1.8 MPa, creating a pressure gradient (~2 MPa) over a specific measurement duration (20 – 60 minutes). This measurement process was repeated for nine points until a steady state measurement became unfeasible due to the sample starting to absorb water without exchanging between the top and bottom paths (Figure 7). A fast change in the apparent permeability to synthetic water was noted, highlighting the material's substantial self-sealing capability. If the gas permeability data is considered as an indication of water permeability without swelling, there is a three-order-of-magnitude decrease in permeability, from approximately 10^{-14} to 10^{-17} m². The rapid change in water permeability underscores the substantial self-sealing capacity of fractures in Opalinus Clay material. Upon inundation, the fracture collapses ($\Delta a<0$, meaning fracture closure) and subsequently swells ($\Delta a>0$, meaning fracture opening) due to further hydration of clay particles. This wetting-induced collapse mechanism is commonly anticipated in the infiltration of geomaterials under confined conditions (Ferber et al., 2008; Seiphoori et al., 2022).

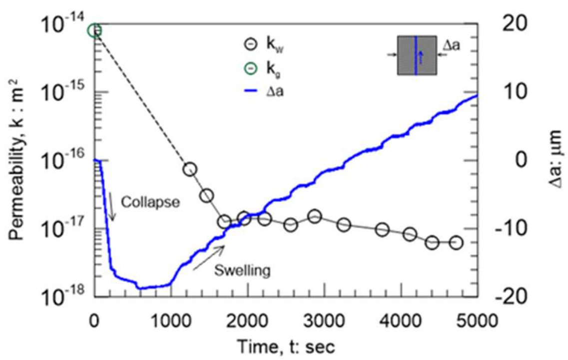

Figure 7. Transition of fracture permeability during the water flow and the deformation measured normal to the fracture plane.

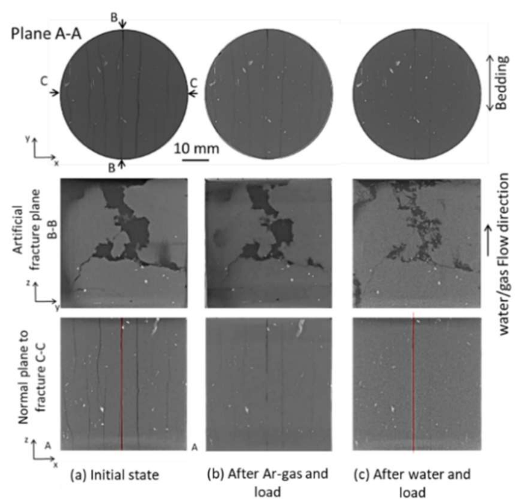

Figure 8. Evolution of fracture plane patterns after loading under gas and after water flows shows how swelling can modify the pore channels by infilling (plugging) them during hydration.

We used the microfocus X-ray CT technique at various stages of gas and water permeability experiments to visualize the evolution of the internal fracture network, showcasing a notable self-sealing behavior associated with swelling of the clay matrix within the fracture planes upon hydration (Figure 8). We acknowledge that the X-ray CT images were captured after the release of confining pressure at each stage, potentially leading to the opening of some fractures compared to when the sample was under load. Nonetheless, the images show the process of fracture closure upon stress application and hydration indicating mechanisms conducive to sealing.

4. Conclusions

Opalinus Clay, a potential host formation for geological disposal of high-level radioactive waste in Switzerland, is typically assumed to restrict the flow of liquids, gases, and particles due to its low permeability (i.e., 10^{-20} to 10^{-21} m^2) and retention properties; however, natural, or excavation-induced fractures can alter this behavior.

Our study reveals several key findings regarding fracture permeability and self-sealing capacity of Opalinus Clay under triaxial stress conditions, due to compaction/consolidation, creep, or via swelling of clay minerals due to re-saturation. Notably, the fracture permeability to gas diminishes with increasing confining stress, where the effect is further pronounced over time due to inelastic deformation of asperities and gouge production, commonly known as fracture creep. We showed the hydration and swelling of the constituting clay aggregates play a pivotal role, leading to a three-order-of-magnitude reduction in fracture permeability. This reduction is attributed to the presence of active clay minerals (illite-smectite mixed layer) and associated swelling deformations causing the fracture geometry to evolve significantly, also visualized through the application of X-ray computed tomography at different stages of the experiment.

The complex processes involved in active fractures demand a comprehensive understanding of material composition and structure, fracture origin, and hydro-chemo-mechanical coupled processes contributing to the swelling of clay aggregates. One key aspect of geological disposal of radioactive waste is related to the generation of gases associated with corrosion and degradation of waste that can cause an excessive pressure build-up and reactivation of sealed fractures (Diomidis et al., 2016). Further research is necessary to determine the gas permeability of fractured clayey rocks post-re-saturation and the self-sealing of fractures. Furthermore, further studies are needed to explore the impact of low isotropic effective stress levels (low confining pressure or large pore pressure) and the more complex stress states associated with deviatoric stresses and creep on the self-sealing of fractures applied in hydrocarbon reservoirs, carbon sequestration, and nuclear waste containment. Once these mechanisms are understood, they can be integrated into predictive models utilized for evaluating the long-term performance of repositories.

Acknowledgments

The first author is grateful for the financial support provided by the National Cooperative for Radioactive Waste Disposal in Switzerland (NAGRA). The Rock Mechanics Laboratory of MIT Department of Earth, Atmospheric, and Planetary Sciences (EAPS) and the MIT Institute for Soldier Nanotechnology are acknowledged for the use of various advanced testing and material characterization equipment.

References

Bock, H. "RA experiment rock mechanics analyses and synthesis: Data report on rock mechanics." Mont Terri Project: Technical Report 2 (2000): 2001.

Bock, Helmut, Boris Dehandschutter, C. Derek Martin, Martin Mazurek, Antoine de Haller, Frédéric Skoczylas, and Catherine Davy. "Self-sealing of fractures in argillaceous formations in the context of geological disposal of radioactive waste." OECD/NEA Report 6184 (2010): 310.

Bossart, Paul. "Twenty years of research at the Mont Terri rock laboratory: what we have learnt." Mont Terri Rock Laboratory, 20 Years: Two Decades of Research and Experimentation on Claystones for Geological Disposal of Radioactive Waste (2018): 407-413.

Diomidis, N., V. Cloet, O. X. Leupin, P. Marschall, A. Poller, and M. Stein. Production, consumption and transport of gases in deep geological repositories according to the Swiss disposal concept. No. NTB-16-03. National Cooperative for the Disposal of Radioactive Waste (NAGRA), 2016.

Elkhoury, Jean E., Russell L. Detwiler, and Pasha Ameli. "Can a fractured caprock self-heal?." Earth and Planetary Science Letters 417 (2015): 99-106.

Ferrari, Alessio, Valentina Favero, and Lyesse Laloui. "One-dimensional compression and consolidation of shales." International Journal of Rock Mechanics and Mining Sciences 88 (2016): 286-300.

Ferber, Valery, Jean-Claude Auriol, Yu-Jun Cui, and Jean-Pierre Magnan. "Wetting-induced volume changes in compacted silty clays and high-plasticity clays." Canadian Geotechnical Journal 45, no. 2 (2008): 252-265.

Johnson, L., P. Marschall, P. Zuidema, and P. Gribi. Effects of post-disposal gas generation in a repository for spent fuel, high-level waste and long-lived intermediate-level waste sited in Opalinus clay. No. NTB--04-06. National Cooperative for the Disposal of Radioactive Waste (NAGRA), 2004.

Hofmann, Hannes, Guido Blöcher, Harald Milsch, Tayfun Babadagli, and Günter Zimmermann. "Transmissivity of aligned and displaced tensile fractures in granitic rocks during cyclic loading." International Journal of Rock Mechanics and Mining Sciences 87 (2016): 69-84.

Mäder, U.J.N.A. (2011): Recipe and preparation of a simplified artificial pore water for Opalinus Clay and Brown Dogger. 11-159.

Marschall, Paul, Marc Distinguin, Hua Shao, Paul Bossart, Chr Enachescu, and Thomas Trick. "Creation and evolution of damage zones around a micro tunnel in a claystone formation of the Swiss Jura Mountains." In SPE International Conference and Exhibition on Formation Damage Control, pp. SPE-98537. SPE, 2006.

Marschall, Paul, Silvio Giger, Rémi De La Vassière, Hua Shao, Helen Leung, Christophe Nussbaum, Thomas Trick et al. "Hydro-mechanical evolution of the EDZ as transport path for radionuclides and gas: insights from the Mont Terri rock laboratory (Switzerland)." Mont Terri Rock Laboratory, 20 Years: Two Decades of Research and Experimentation on Claystones for Geological Disposal of Radioactive Waste (2018): 175-196.

Mazurek, Martin, Anthony J. Hurford, and Werner Leu. "Unravelling the multi-stage burial history of the Swiss Molasse Basin: integration of apatite fission track, vitrinite reflectance, and biomarker isomerisation analysis." Basin Research 18, no. 1 (2006): 27-50.

Mazurek, Martin, Andreas Gautschi, Paul Marschall, Georges Vigneron, Patrick Lebon, and Jacques Delay. "Transferability of geoscientific information from various sources (study sites, underground rock laboratories, natural analogues) to support safety cases for radioactive waste repositories in argillaceous formations." Physics and Chemistry of the Earth, Parts A/B/C 33 (2008): S95-S105.

Raven, K. G., and J. E. Gale. "Water flow in a natural rock fracture as a function of stress and sample size." In International Journal of Rock Mechanics and Mining Sciences & Geomechanics, vol. 22, no. 4, pp. 251-261. Pergamon, 1985.

Seiphoori, Ali, Andrew J. Whittle, Konrad J. Krakowiak, and Herbert H. Einstein. "Insights into diagenesis and pore structure of Opalinus shale through comparative studies of natural and reconstituted materials." Clays and Clay Minerals 65 (2017): 135-153.

Seiphoori, Ali, and Mostafa Zamanian. "Improving mechanical behaviour of collapsible soils by grouting clay nanoparticles." Engineering Geology 298 (2022): 106538.

Tsang, Chin-Fu, Jens Birkholzer, and Jonny Rutqvist. "A comparative review of hydrologic issues involved in geologic storage of CO2 and injection disposal of liquid waste." Environmental Geology 54 (2008): 1723-1737.